Observational Study

Medicine®

OPEN

Heterogeneity analysis of triphasic CT scan perfusion parameters in differential diagnosis of hepatocellular carcinoma and hemangioma

Guodong Pang, MD[a], Zuyun Duan, MM[b], Chunchun Shao, MM[c], Fang Zhao, PhD[d], Hai Zhong, MD[a], Guangrui Shao, PhD[a,*]

Abstract

This study is to investigate quantitative measures and heterogeneity of perfusion parameters in the differential diagnosis of hepatocellular carcinoma (HCC) and hemangioma.

In total, 32 HCC and 44 hemangioma (types 1, 2, and 3) cases were included in this retrospective study. Hepatic artery coefficient (HAC), portal vein coefficient (PVC), and arterial enhancement fraction (AEF) were calculated. Tumor heterogeneity was analyzed. Perfusion parameters and corresponding percentiles were compared between the HCC and hemangioma (especially atypical hemangioma) cases, as well as between the substantial lesion part and surrounding normal tissue.

The mean value, and the 10th, 50th, 75th, and 90th percentiles of PVC were significantly lower in the HCC cases than the types 1 and 2 hemangioma cases ($P < .01$). Moreover, the 90th percentile PVC in the HCC cases was also significantly lower than the type 3 hemangioma case ($P < .01$), while the mean value, and all the percentiles of AEF in the HCC cases were higher than the types 2 and 3 hemangioma cases ($P < .01$). The 10th percentile HAC in the HCC cases was higher than the type 2 hemangioma cases ($P < .05$). The mean value, and the 10th and 50th percentile HAC in the HCC cases were higher than the type 3 hemangioma case ($P < .05$). However, there was no statistically significant difference in HAC between the HCC and type 1 hemangioma cases ($P > .05$).

Quantitative measurement of perfusion parameters and heterogeneity analysis show significance differences in the early detection and differential diagnosis of HCC and hemangioma cases, which might contribute to increasing the diagnostic accuracy.

Abbreviations: AEF = arterial enhancement fraction, CT = computed tomography, HAC = hepatic artery coefficient, HCC = hepatocellular carcinoma, ICC = intraclass correlation coefficients, MRI = magnetic resonance imaging, PVC = portal vein coefficient, ROIs = regions of interest.

Keywords: computed tomography perfusion imaging, hemangioma, hepatocellular carcinoma, heterogeneity analysis, histogram analysis

1. Introduction

Hepatocellular carcinoma (HCC) is one of the most common hepatic malignant hepatic tumors in clinic, which primarily occurs in patients with chronic hepatitis or cirrhosis.[1–4] Early detection of HCC has been extremely important for the successful therapy of the local tumors. Of the early detected HCC cases, up to 90% of the patients could be cured under the best circumstances.[5,6] According to the European Association for the Study of Liver Diseases 2000 Conference[7] and American Association for the study of Liver Diseases guidelines,[8] diagnosis of HCC based on conventional enhancement computed tomography (CT) relies on the observation of arterial enhancement, which is followed by the contrast washout in the venous phase.[9] However, the HCC lesions <20 mm are always difficult to diagnose due to the specific vascularization pattern and the complicated liver texture with cirrhotic background.[1,10–12] Besides, not all HCC cases report the contrast washout on the portal venous phase and delayed imaging. A minority of the well-differentiated HCC cases would be hypodense to the liver on all phases.[13] Moreover, washout could also be performed in other focal liver lesions, including hemangioma, focal nodular hyperplasia, and hypervascular metastases.[14]

Hepatic hemangioma represents the most common benign liver tumor, with the prevalence of 0.4% to 20%.[15] Typical hemangioma is easily differentiated with HCC. However, atypical appearance of hepatic hemangioma is commonly seen in daily practice, such as large heterogeneous hemangioma (type 3) and rapidly filling hemangioma (type 1).[16,17] The atypical features may lead to misdiagnosis and confusion with other lesions. For example, small hemangioma lesions may show arteriovenous shunting, and hemangiomas <1 cm would have rapid filling. Differential diagnosis between atypical hemangioma and HCC has been considered to be difficult.[18]

Editor: Jianxun Ding.

This work was funded by the Project of Youth Fund in our hospital (No. Y2013010059).

The authors have no conflicts of interest to disclose.

[a] Department of Radiology, The Second Hospital of Shandong University, Jinan, [b] Department of Radiology, The Second People's Hospital of Dongying, Dongying, [c] Department of Evidence-Based Medicine, The Second Hospital of Shandong University, [d] Department of Radiology, Qilu Hospital of Shandong University, Jinan, Shandong, China.

[*] Correspondence: Guangrui Shao, Department of Radiology, The Second Hospital of Shandong University, No. 247, Beiyuan Road, Jinan, Shandong 250033, China (e-mail: guangrui1963@sina.com).

Medicine (2018) 97:38(e12512)

Received: 23 April 2018 / Accepted: 29 August 2018

http://dx.doi.org/10.1097/MD.0000000000012512

CT perfusion imaging represents important assessment method for tumor-related vascularization. CT perfusion could measure the hemodynamic parameters at the capillary level, with high temporal and spatial resolution, as well as good reproducibility, which therefore plays an important role in the early diagnosis of HCC. The perfusion parameters could quantitatively reflect the hemodynamic changes in microcirculation, which provides morphological and functional information of the target lesions. However, the CT perfusion has 2 major limitations, that is, the large radiation dose and the inspiratory or expiratory motion and distortion-induced artifacts.

Tumor heterogeneity is determined by the heterogeneous vascularization, necrosis, fibrosis, and cell density. Considering the lesion tissue structure, there may be some evident differences between the HCC and hemangioma or normal parenchyma. Previous studies on the quantitative images of tumor vascularization have reported the average perfusion parameters, disregarding the perfusion heterogeneity. One way to assess the variable tumor perfusion is the histogram analysis, which yields several parameters, including the coefficient of variation, percentiles, skewness, and kurtosis. The histogram analysis of apparent diffusion coefficient maps has great value in predicting the aggressiveness of endometrial cancer, prostate cancer, and bladder cancer.[19–21] Percentiles have been reported to be more robust than other histogram analysis parameters. Various percentiles are quite insensitive to distortion of the histogram shape by the peaks.[22] Therefore, the differential diagnostic performance between HCC and hemangioma might be improved by using the histogram analysis of perfusion parameters (mainly using the percentiles). The present study was designed to investigate the variance of perfusion parameters by histogram analysis in the HCC and liver benign hemangioma cases. The CT perfusion parameters and percentiles of hemangioma cases (typical and atypical) were calculated, according to enhancement pattern, in comparison with HCC. The feasibility of quantitative measurement of perfusion parameters and heterogeneity assessment by the histogram analysis in the differential diagnosis between HCC and hemangioma (especially atypical cases) was evaluated.

2. Materials and methods

1.1. Study patients

In total, 84 liver lesions (in 76 patients) were included in the study group, including 38 HCC and 46 hemangioma cases. HCC cases were confirmed by biopsy and resection, while the diagnosis of hemangioma was based on the radiology reports (including follow-up studies) or biopsy. Small and atypical hemangioma had to meet all of the following criteria: resolution on the follow-up imaging, normal alpha fetoprotein, and no suspicious features on magnetic resonance imaging (MRI). The mean diameter of these 38 HCC lesions was 3.6 ± 2.7 cm, ranging from 1.5 to 11.4 cm. The mean diameter of these 46 hemangioma cases was 2.5 ± 1.4 cm, ranging from 1.3 to 5.9 cm. In the 32 patients with 38 HCC lesions, there were 19 lesions in the left lobe of the liver, 16 lesions in the right lobe, and 3 lesions in both these 2 lobes. In the 44 patients with 46 hemangioma lesions, there were 20 lesions in the right lobe and 26 lesions in the left lobe. Inclusion criteria were as follows: confirmation from the pathology, transplant for HCC, or contrast-enhanced CT and MRI with classic imaging features during the follow-up period; availability of triple-phase contrast-enhanced CT scans obtained with the identical scanning and contrast injection protocol; having no previous treatment, such as liver surgery, chemotherapy, chemoembolization therapy, or liver radiotherapy, within 6 weeks; and having adequate renal function (serum creatinine level ≤ 2.0 mg/dL). The exclusion criteria were as follows: patients with portal vein thrombosis or portal vein tumor thrombosis for HCC; patients with allergy, or contraindication to the use of contrast; patients with severe heart diseases; or the arterially enhancing portion of the lesion was too small to characterize (≤ 5 mm). Of these 76 patients, there were 29 patients with cirrhosis, as diagnosed by pathology or the CT appearance, including 20 cases of viral hepatitis type B, 7 cases of alcoholic liver disease, and 2 patients with unknown reasons. This retrospective study was approved by the Institutional Review Board of our hospital. Written informed consent was obtained from all patients, according to the guidelines of the local ethics committee.

1.2. CT scanning protocol and CT perfusion analysis

All patients were subjected to the examination using a 128-slice CT scanner system (GE Discovery CT750 HD, Waukesha, WI). At 15 minutes before the CT scanning, patients were required to drink 500 mL water to fill the gastrointestinal tract. For the enhancement, 100 mL iodinated contrast (Omnipaque 350 mg iodine/mL; GE) was injected intravenously, at a rate of 3.5 to 4.5 mmL/s. After the unenhanced CT scanning, the arterial phase (30–35 seconds), portal venous phase (60–70 seconds), and delayed phase (180 seconds) were performed after the start of contrast injection. Scanning parameters were as follows: collimation, 128×0.625 mm; tube voltage, 80 to 120 kV; effective tube current time product, 200 mA; and pitch, 1.375.

The CT hemodynamic kinetics software (GE Healthcare, HD750) was used for data analysis, and the liver perfusion parameters include the hepatic artery supply coefficient (HAC), portal vein blood supply coefficient (PVC), and arterial enhancement fraction (AEF). These parameters provide a simple way to quantitatively characterize the enhancement curves on the triple-phase liver CT scanning. HAC and PVC described the enhancement curve for a liver lesion as a linear combination of the aortic and portal venous enhancement curves. HAC indicated the similarity of lesion's enhancement curve to the aortic enhancement curve, and PVC manifested the similarity of lesion's enhancement curve to the portal venous enhancement curve. HAC and PVC were equal to aortic and portal vein blood volumes, in a simple perfusion model that assumed rapid blood flow and no vascular permeability. For each tumor, regions of interest (ROIs) were drawn over the tumor, portal vein, and aorta on images, in which the calculation involved measurements of mean attenuation. HAC = (v2x1 + v2x2 + v3x3)/(a2v3 − a3v2) and PVC = (a2x1 + a2x2 + a3x3)/(a3v2 − a2v3), where xi was the enhancement of the pixel in the liver, ai was the enhancement of the aorta, and vi was the enhancement of the portal vein. Moreover, i = 1 was the arterial phase, i = 2 was the portal venous phase, and i = 3 was the delayed phase. Enhancement was measured in the Hounsfield units, relative to the average Hounsfield units of the 3 phases.[14] AEF was defined as the ratio of the absolute increment of attenuation during the arterial phase to the absolute increment of attenuation during the portal venous phase: $AEF = [(HUa - HUu)/(HUp - HUu)] \times 100$, where HU was the attenuation, a was the arterial phase, p was the portal phase, and u was unenhanced.[9,23]

1.3. Imaging analysis

Hemangioma cases were usually classified into 3 enhancement types[16]: type 1, early complete or almost complete enhancement

Table 1

Relative enhancement pattern of target lesions.

Enhancement type		N
HCC	Hypervascular with wash out	30
	Hypodense on all phases	2
Hemangioma	Type 1	12
	Type 2	20
	Type 3	12

HCC = hepatocellular carcinoma.

during the arterial phase, with iso- or hyperdensity compared with surrounding parenchyma; type 2, peripheral nodular enhancement during the arterial phase, and progressive filling-in on the portal venous or delayed images; and type 3, peripheral nodular enhancement type during the arterial phase, without complete filling on the delayed phases. The HCC lesions were presented as hypervascular with washout or hypodense on all phases (Table 1; Figs. 1–3).

Breathing motion was compensated by nonrigid image registration if necessary. ROIs were manually placed in the aorta and portal vein to measure the arterial and portal venous input. The whole liver perfusion parameters were calculated and mapped into the color-coded parametric maps. All examinations were reviewed by 2 radiologists (a resident with 2 years and a radiologist with 8 years of experience). For each patient, the radiologists manually delineated the ROI around the entire section of the tumor. ROIs were also placed on the hepatic parenchyma of tumor-free regions, excluding the large intrahepatic vessels.

1.4. Statistical analysis

The Graph Pad Prism software was used for statistical analysis. All data were tested for normal distribution by the Kolmogorov–Smirnov test. Interobserver agreement with respect to quantitative perfusion parameters of the target lesions was evaluated with the intraclass correlation coefficients (ICC). Agreement degrees were categorized as follows: 0.00 to 0.39, poor agreement; 0.40 to 0.59, fair agreement; 0.60 to 0.74, good agreement; and 0.75 to 1.00, excellent agreement.[24] For each lesion, the perfusion parameters (HAC, PAC, and AEF) were obtained automatically from the tri-phases enhancement scanning, which were analyzed voxel-by-voxel using the histogram analysis. The 10th, 50th, 75th, and 90th percentiles of histogram parameters were analyzed. The intragroup perfusion parameters and histogram parameters were compared using the paired sample t test. The Intergroup perfusion and histogram parameters' measurements were compared by the 2-sample independent t test. Multiple group differences were compared with analysis of variance. $P < .05$ was considered statistically significant.

3. Results

1.5. Interobserver agreement

Perfusion parameters of the lesions in the ROIs showed excellent interobserver agreement for the mean value and the percentiles of histogram parameter, with the ICC value of 0.91. Therefore, the measurement data from these 2 observers were suitable for the following analysis.

1.6. Comparison of perfusion parameters and percentiles between HCC and surrounding liver parenchyma

The perfusion parameters and percentiles were compared between the HCC lesion and surrounding liver parenchyma. Our results showed that the mean value, and the 10th, 50th, 75th, and 90th percentiles of HAC and AEF were significantly higher than the surrounding liver parenchyma ($P < .05$), while the mean value, and the 10th, 50th, 75th, and 90th percentiles of PVC were significantly lower in the HCC cases than the surrounding liver parenchyma ($P < .01$) (Table 2; Fig. 4). These results suggest that the mean value and percentiles of HAC and AEF in HCC are significantly higher than the surrounding liver parenchyma, while the mean value and percentiles of PVC in HCC are significantly lower than the in surrounding liver parenchyma.

1.7. Comparison of perfusion parameters and percentiles between HCC and hemangiomas

The perfusion parameters and percentiles were compared between the HCC lesions and hemangiomas. Our results showed that the mean value, and all the percentiles of PVC were significantly lower in the HCC tumor tissue than the types 1 and 2 hemangioma showing hypoperfusion ($P < .01$); and the 90th percentile of PVC in the HCC cases was also significantly lower than the type 3

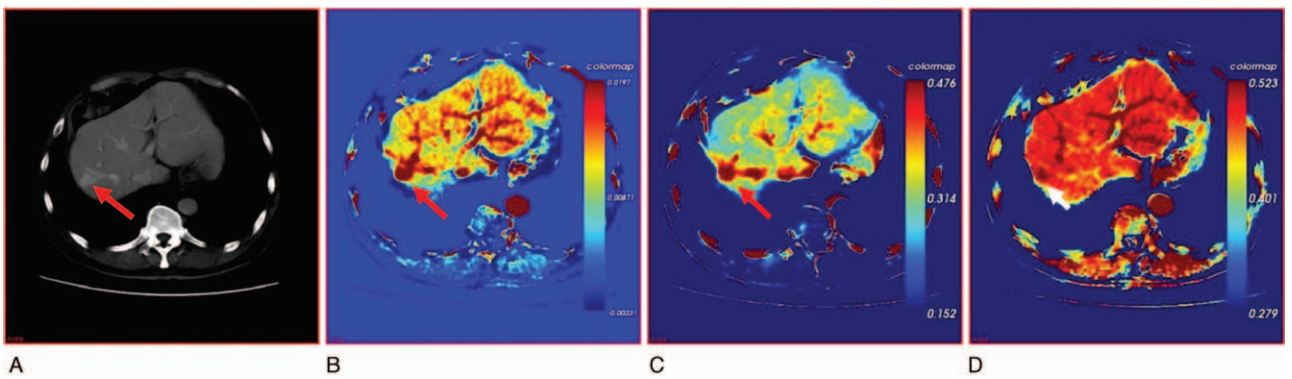

Figure 1. Perfusion image of type 1 hemangioma in a 35-year-old male patient. (A) Raw data depicting small round lesion in right liver lobe with nodular enhancement on arterial phase (red arrow). HAC (B), PVC (C), and AEF (D) images all showing homogeneous hyperperfusion (red arrow). AEF = arterial enhancement fraction, HAC = hepatic artery coefficient, PVC = portal vein coefficient.

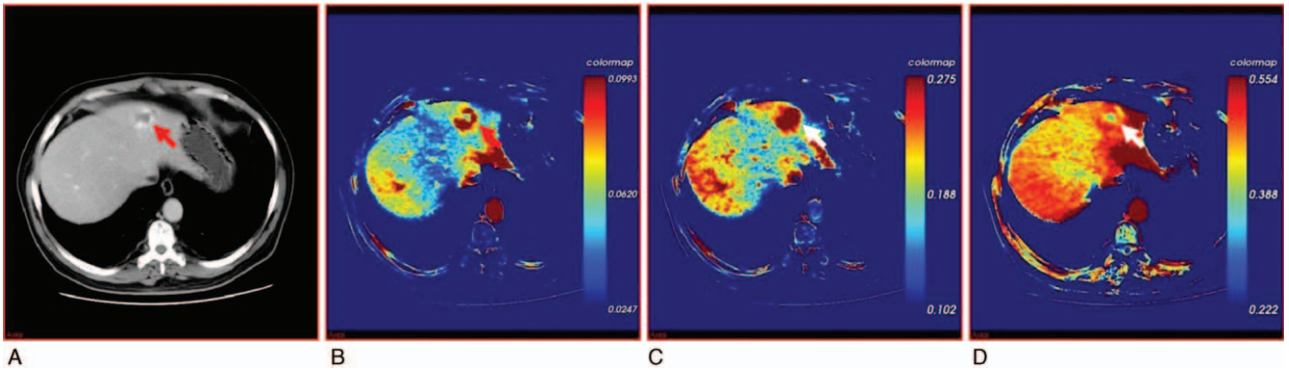

Figure 2. Perfusion image of type 2 hemangioma in a 46-year-old female patient. (A) Raw data showing round lesion in left liver lobe with nodular enhancement in the rim and hypoattenuation in the center (red arrow). (B) HAC image showing higher perfusion in the rim and lower perfusion in the center (red arrow). (C) PVC image showing hyperperfusion in the entire lesion (red arrow). (D) AEF image showing higher perfusion in the rim and lower perfusion in the center (red arrow). AEF = arterial enhancement fraction, HAC = hepatic artery coefficient, PVC = portal vein coefficient.

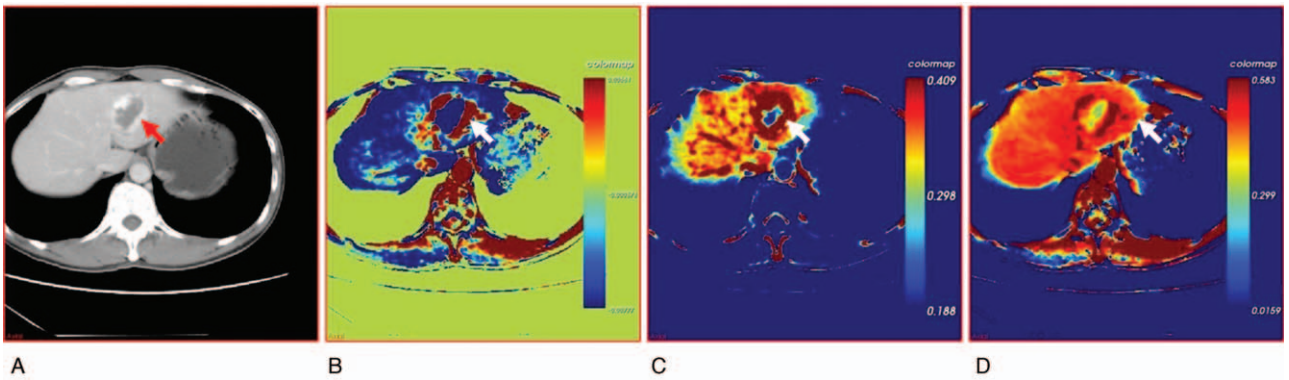

Figure 3. Perfusion image of type 3 hemangioma in a 52-year-old male patient. (A) Raw data showing round lesion in the left liver lobe with nodular enhancement in the rim and hypoattenuation in the center (red arrow). HAC (B) and AEF (C) images showing hyperperfusion in the rim and hypoperfusion in the center (red arrow). (D) PVC image also depicting higher perfusion in the rim and lower perfusion in the center, with larger range of hyperperfusion than HAC image, in line with enhancement pattern (red arrow). AEF = arterial enhancement fraction, HAC = hepatic artery coefficient, PVC = portal vein coefficient.

Table 2

Comparison of CT perfusion parameters and percentiles between HCC and surrounding liver parenchyma.

	HAC			PVC			AEF		
	HCC	Liver parenchyma	*P*	HCC	Liver parenchyma	*P*	HCC	Liver parenchyma	*P*
Mean ± SD	0.019 ± 0.030	−0.0042 ± 0.041	.0178	0.23 ± 0.064	0.35 ± 0.090	<.0001	0.62 ± 0.10	0.48 ± 0.035	<.0001
10th percentile	0.0077 ± 0.033	−0.0093 ± 0.042	.0845	0.17 ± 0.075	0.31 ± 0.087	<.0001	0.53 ± 0.13	0.45 ± 0.036	<.0001
50th percentile	0.019 ± 0.030	−0.0043 ± 0.041	.0165	0.23 ± 0.065	0.35 ± 0.090	<.0001	0.61 ± 0.088	0.48 ± 0.035	<.0001
75th percentile	0.026 ± 0.028	−0.0016 ± 0.040	.0028	0.26 ± 0.061	0.36 ± 0.092	<.0001	0.65 ± 0.096	0.49 ± 0.035	<.0001
90th percentile	0.031 ± 0.028	0.0011 ± 0.040	.0008	0.29 ± 0.060	0.38 ± 0.094	<.0001	0.70 ± 0.12	0.50 ± 0.037	<.0001

AEF = arterial enhancement fraction, CT = computed tomography, HAC = hepatic artery coefficient, HCC = hepatocellular carcinoma, PVC = portal vein coefficient, SD = standard deviation.

hemangioma ($P < .01$). However, the mean value and all the percentiles of AEF in the HCC cases were significantly higher than the types 2 and 3 hemangioma showing hyperperfusion ($P < .01$). Moreover, the 10th percentile of HAC in the HCC cases was higher than the type 2 hemangioma ($P < .05$). Furthermore, the mean value, and the 10th and 50th percentiles of HAC in the HCC cases were higher than the type 3 hemangioma ($P < .05$) (Table 3; Figs. 5 and 6). These results suggest that the mean value and percentiles of PVC are significantly lower in the HCC cases than the types 1 and 2 hemangioma cases, while the mean value and percentiles of AEF in the HCC cases are higher than the types 2 and 3 hemangioma cases.

4. Discussion

The CT perfusion imaging is a kind of functional imaging technique in which a quantitative map is created characterizing the tumor microcirculation and hemodynamic changes. However, the clinical application of CT perfusion imaging has not been

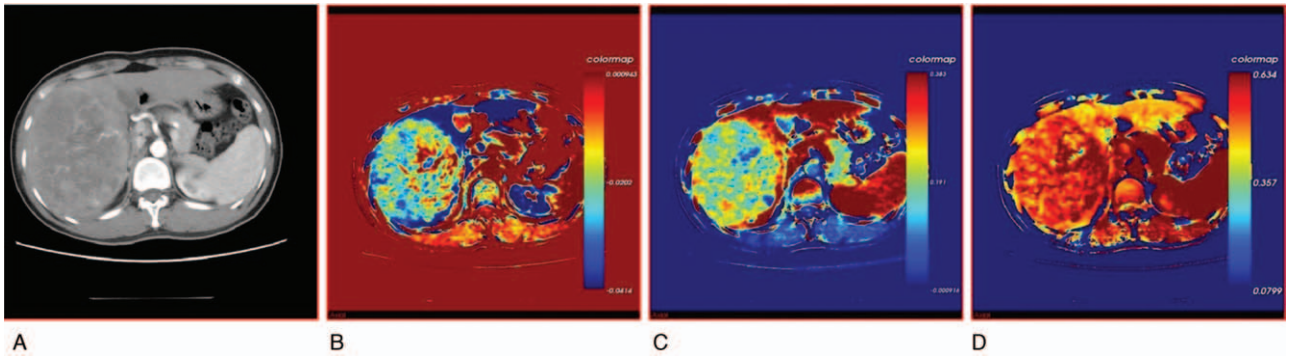

Figure 4. Perfusion image of HCC in a 58-year-old female patient with jaundice. (A) Raw data showing giant lesion in right liver lobe with obviously uneven reinforcement. (B) HAC image depicting high perfusion in the lesions with heterogeneity. (C) PVC image showing hypoperfusion lesion. (D) AEF image showing heterogeneous hyperperfusion in the entire lesion. AEF = arterial enhancement fraction, HAC = hepatic artery coefficient, HCC = hepatocellular carcinoma, PVC = portal vein coefficient.

fully realized. There might be 2 major reasons, that is, the unclear clinical role and the increased radiation dose. In this study, the CT kinetic hemodynamic software was used, based on a simplified model of tumor blood supply, which would be applied to the traditional triphasic scanning. Thus, the radiation dose was significantly reduced, compared with the conventional CT perfusion scanning.[14] Our results showed the significant different perfusion parameters, as well as 10th, 50th, 75th, and 90th percentiles of histogram between the HCC and hemangioma cases for the disease differentiation. Atypical and typical hemangioma could be easily differentiated with HCC. In a previous study, the most arterially enhancing part of the lesion has been measured in the heterogeneous lesions. However, the choice of ROI was still somewhat arbitrary.[14] In the present study, for each patient, the radiologists manually delineated the ROIs around the entire section of the tumor to eliminate bias, which might provide more accurate and objective results.

This is the first study focusing on the assessment of perfusion parameters and heterogeneity between the HCC and hemangioma cases of different enhancement patterns. Singh et al[25] and Guo and Yu[26] have reported differential CT perfusion values between the HCC and hemangioma cases. However, in these studies, the hemangioma cases have not been classified into different enhancement patterns, or atypical and typical types, which might lead to bias and mirror results. In this study, hemangioma with different enhancement patterns had different CT perfusion parameters. Furthermore, they did not refer to the percentiles of histogram analysis. Our results showed that it was important to take the tumor heterogeneity into account, for the differentiating diagnosis between HCC and hemangiomas, by using the histogram analysis. Tumor heterogeneity was determined by the cell density, necrosis, heterogeneous vascularization, and fibrosis.[27] Histogram analysis was an effective method to assess the tumor heterogeneity. Among these quantitative parameters derived from histogram analysis, percentiles have thought to be more robust than others.[22] Therefore, percentiles were applied herein for the heterogeneity analysis of HCC and hemangioma cases. Our results showed that the percentiles of histogram analysis played important roles in differentiating HCC and hemangioma cases. For example, only the 10th percentile of HAC from the voxel-wise histogram analysis of HCC was significantly higher than the type 2 hemangioma. By contrast, the mean value and the other percentiles of HAC in tumors did not show significant difference between HCC and type 2 hemangioma. These results indicated the

Table 3

Comparison of CT perfusion parameters and percentiles between HCC and hemangiomas with different enhancement patterns.

	HCC	Type 1 hemangioma	Type 2 hemangioma	Type 3 hemangioma	*P* (HCC vs type 1)	*P* (HCC vs type 2)	*P* (HCC vs type 3)
HAC, mean ± SD	0.019 ± 0.030	0.023 ± 0.024	−0.010 ± 0.062	−0.0025 ± 0.027	.8433	.0853	.0226
10th percentile	0.0077 ± 0.033	0.011 ± 0.027	−0.036 ± 0.070	−0.023 ± 0.029	.8433	.0165	.0054
50th percentile	0.019 ± 0.030	0.023 ± 0.023	0.012 ± 0.061	−0.0035 ± 0.025	.8433	.0563	.0184
75th percentile	0.026 ± 0.028	0.030 ± 0.023	0.0035 ± 0.059	0.0073 ± 0.027	.9685	.0770	.0626
90th percentile	0.031 ± 0.028	0.035 ± 0.022	0.017 ± 0.059	0.019 ± 0.032	.9895	.2390	.2058
PVC, mean ± SD	0.23 ± 0.064	0.34 ± 0.092	0.38 ± 0.12	0.25 ± 0.096	<.0001	<.0001	.5573
10th percentile	0.17 ± 0.075	0.30 ± 0.087	0.28 ± 0.095	0.12 ± 0.081	<.0001	<.0001	.0632
50th percentile	0.23 ± 0.065	0.34 ± 0.097	0.38 ± 0.12	0.23 ± 0.11	<.0001	<.0001	.9386
75th percentile	0.26 ± 0.061	0.37 ± 0.098	0.44 ± 0.14	0.31 ± 0.10	<.0001	<.0001	.0703
90th percentile	0.29 ± 0.060	0.39 ± 0.098	0.48 ± 0.15	0.39 ± 0.11	.0002	<.0001	.0005
AEF, mean ± SD	0.62 ± 0.10	0.63 ± 0.12	0.53 ± 0.087	0.43 ± 0.052	.8433	.0003	<.0001
10th percentile	0.53 ± 0.13	0.59 ± 0.10	0.45 ± 0.084	0.28 ± 0.092	.2305	.0005	<.0001
50th percentile	0.61 ± 0.088	0.63 ± 0.12	0.52 ± 0.085	0.44 ± 0.044	.9895	.0003	<.0001
75th percentile	0.65 ± 0.096	0.66 ± 0.14	0.57 ± 0.099	0.50 ± 0.055	.9551	.0034	<.0001
90th percentile	0.70 ± 0.12	0.68 ± 0.14	0.61 ± 0.11	0.56 ± 0.078	.5510	.0061	.0001

AEF = arterial enhancement fraction, CT = computed tomography, HAC = hepatic artery coefficient, HCC = hepatocellular carcinoma, PVC = portal vein coefficient, SD = standard deviation.

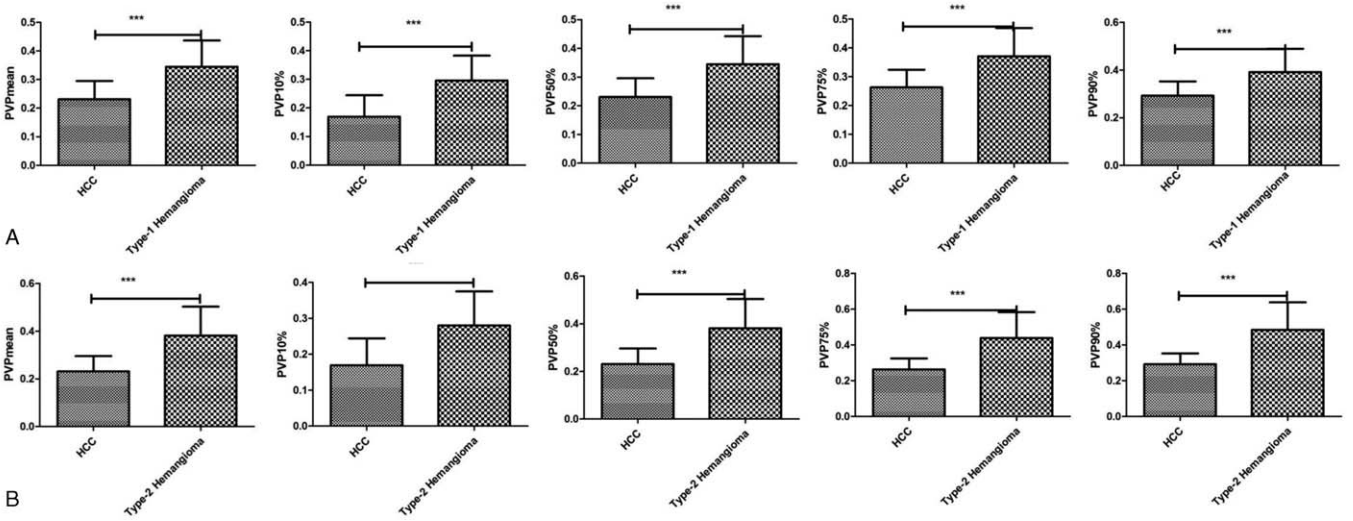

Figure 5. Graphs of PVC ranging from the mean value to 10th to 90th percentiles of HCC and hemangioma. Significant difference in the mean value and percentiles of PVC between HCC and types 1 (A) and 2 (B) hemangioma cases. Compared with the HCCs, $^{*}P < .05$, $^{**}P < .01$. HCC = hepatocellular carcinoma, PVC = portal vein coefficient.

differences of tumor heterogeneity between these HCC and type 2 hemangioma cases. Previous studies on quantitative imaging have reported the average perfusion values of entire tumors, disregarding the perfusion heterogeneity.[24,25] In this study, the tissue perfusion and the heterogeneity of different tumors were analyzed, and the quantitative perfusion imaging may be more adequate for the differential diagnosis of HCC and hemangiomas.

In the case of typical hemangioma, imaging features are highly reliable for the disease diagnosis. The typical appearance is hypoattenuating on the unenhanced phase, with the type 2 enhancement feature during the enhancement phase. Hemangioma of type 1 enhancement pattern occurs more often in small hemangioma, which shows immediate homogeneous enhancement at the arterial phase in the scanning. It is likely that the smaller the lesion, the more rapid the spread of contrast material within it would be.[28] For the type 3 hemangioma, at the venous and delayed phases, the progressive centripetal enhancement would not lead to complete filling, which has been associated with the central scar.[28,29] Pathologically, the scar is caused by thrombosis, fibrous, myxomatous change, and necrosis.

The development and progression of HCC are characterized by multistep carcinogenesis. The carcinogenesis process might lead to increased arterial liver perfusion (ALP) and decreased PVC, finally resulting in increased AEF due to the damage of normal sinusoidal architecture.[30] Tumor perfusion is usually reported as the mean values of perfusion parameters. Meanwhile, the mean values do not interpret the heterogeneous distribution of tumor perfusion, and thus could not be optimal for the tumor assessment before treatment or therapy evaluation. In this study, not only the mean value of perfusion parameters was analyzed,

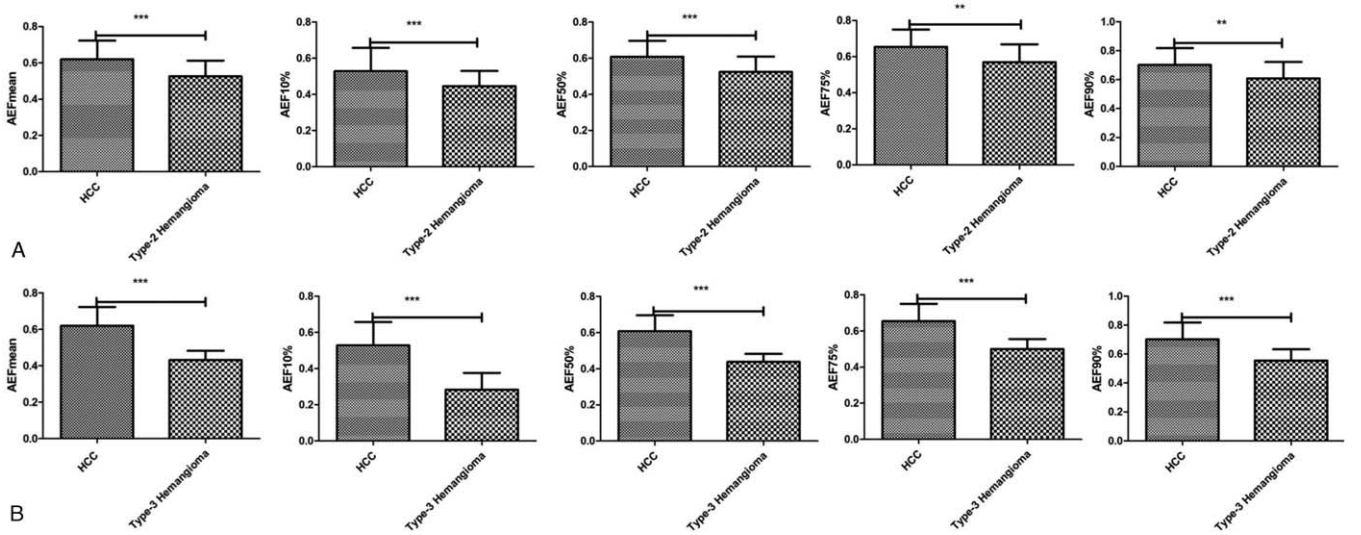

Figure 6. Graphs of AEF ranging from the mean value to 10th to 90th percentiles of HCC and hemangioma. Significant difference in the mean value and different percentiles of PVC between HCC and types 2 (A) and 3 (B) hemangioma cases. Compared with the HCCs, $^{*}P < .05$, $^{**}P < .01$. AEF = arterial enhancement fraction, HCC = hepatocellular carcinoma, PVC = portal vein coefficient.

but also the percentiles of histogram analysis were calculated, which might be superior to median values for tumor grading and tumor recurrence evaluation.[28,31] The mean values, and the 10th, 50th, 75th, and 90th percentiles of HAC and AEF were significantly higher than the surrounding liver parenchyma, whereas the mean value, and the 10th, 50th, 75th, and 90th percentiles of PVC were significantly lower in the HCC tumor than the surrounding liver parenchyma, which was in line with previous findings.[32–34]

Early detection plays a critical role for the successful local tumor surgery.[5,35,36] In the case of typical hemangioma, imaging features are highly credible for the accurate diagnosis.[28] Nevertheless, atypical features in the cases of atypical hemangioma may result in confusion with other lesions and/or misdiagnosis. Therefore, differential diagnosis of atypical hemangioma from HCC is pivotal but challenging. Heterogeneity in enhancement was found in different types of hemangioma or in HCCs. Therefore, the heterogeneity evaluation using the histogram analysis may represent the identifying features between the HCC and hemangioma cases.

In this study, the mean value and percentiles of perfusion parameters were analyzed and compared between HCC and hemangiomas (typical and atypical). The mean value and all the percentiles of AEF were significantly higher than the types 2 and 3 hemangioma showing hyperperfusion, whereas the mean value and all the percentiles of PVC were significantly lower in the HCC tumor tissue than the types 1 and 2 hemangioma showing hypoperfusion. The 90th percentile of AEF in the HCCs was also significantly lower than the type 3 hemangioma, while there was no difference in the mean PVC value, or in the 10th, 50th, and 75th percentiles due to heterogeneous structure in the type 3 hemangioma case. The PVC and AEF values were particularly related to the differential diagnosis of HCC and hemangioma cases, which was in line with previous reports.[26] Moreover, our results were more scientific, rigorous, and accurate, due to the following reasons: First, the hemangiomas were classified into 3 types, according to the enhancement patterns, and the CT perfusion parameters were compared among these 3 types. Second, the histogram analysis was introduced to assess the different types of hemangioma (typical and atypical), to quantify the tumor heterogeneity. Histogram analysis could evaluate the intensity variations within the tumors, evaluating the lesion heterogeneity and architecture feature related to pathology. More importantly, percentiles of perfusion parameters play important roles in the histogram analysis.

There was no statistically significant difference in the liver parenchyma between different types of hemangiomas, and between the HCC and hemangioma. In previous studies, the progression of liver cirrhosis would result in decreased PVC, which is then compensated by the increased HAC, finally leading to increased AEF. In this study, for patients with HCC, tumor-free parenchyma of most patients had cirrhosis. Meanwhile, there was no difference between patients with hemangiomas. This phenomenon could be explained that the patients with cirrhosis were classified into the Child-Pugh A, which did not lead to hemodynamic changes. Other reasons may be due to the different techniques and algorithm used for CT perfusion, or the relative limited sample sizes.

These are several limitations of this study. First, there were some patients without histopathologic proof for the lesions (especially hemangiomas). Second, because the triphasic dynamic CT dataset were extracted from the traditional CT perfusion dataset, the volume, duration, and concentration of contrast injections between triphasic dynamic and traditional CT perfusion scanning may differ, which could alter the perfusion parameters. Third, only the percentiles of histogram analysis were analyzed, while other parameters were not involved, such as skewness, kurtosis, and variance. The study did not comprehensively reflect the tumor heterogeneity. Fourth, there was potential risk of selection bias in the retrospective study. Fifth, our study population was reasonably small, and further studies with enlarged population of patients are still needed.

In conclusion, our results showed that the CT perfusion parameters and percentile analysis of histogram calculated from triphasic liver CT scanning could be used, not only to assess the hemodynamic changes and tumor heterogeneity, among the HCC and hemangiomas (typical and atypical), but also to differentiate hemangioma from HCC using different hemodynamic situation. These coefficients could provide complementary information in addition to the traditional imaging diagnosis criteria (such as washout for HCC, periphery nodular enhancement, and the progress to the central filling for hemangioma), in order to improve the specificity and sensitivity of diagnosis.

Author contributions

Data curation: Zuyun Duan.
Formal analysis: Guodong Pang.
Funding acquisition: Guangrui Shao.
Investigation: Chunchun Shao.
Resources: Hai Zhong.
Software: Fang Zhao.
Writing – original draft: Guodong Pang.
Writing – review & editing: Guangrui Shao.

References

[1] Baron RL, Peterson MS. From the RSNA refresher courses: screening the cirrhotic liver for hepatocellular carcinoma with CT and MR imaging—opportunities and pitfalls. RadioGraphics 2001;21:S117–32.
[2] Baker ME, Pelley R. Hepatic metastases: basic principles and implications for radiologists. Radiology 1995;197:329–37.
[3] Jiang H, Zhang Z, Shen B, et al. Functional CT for assessment of early vascular physiology in liver tumors. Hepatobiliary Pancreat Dis Int 2008;7:497–502.
[4] Waldman SA, Fortina P, Surrey S, et al. Opportunities for near-infrared thermal ablation of colorectal metastases by guanylyl cyclase C—targeted gold nanoshells. Future Oncol 2006;2:705–16.
[5] Sherman M, Bruix J, Porayko M, et al. Screening for hepatocellular carcinoma: the rationale for the American Association for the Study of Liver Diseases recommendations. Hepatology 2012;56:793–6.
[6] Duran R, Chapiro J, Schemthaner RE, et al. Systematic review of catheter-based intra-arterial therapies in hepatocellular carcinoma state of the art and future directions. Br J Radiol 2015;88:20140564.
[7] Bruix J, Sherman M, Llovet JM, et al. Clinical management of hepatocellular carcinoma: conclusions of the Barcelona-2000 European Association for the Study of the Liver conference. J Hepatol 2001;35: 421–30.
[8] Bruix J, Sherman M. Management of hepatocellular carcinoma: an update. Hepatology 2011;53:1020–2.
[9] Kyung WK, Jeong ML, Ernst K, et al. Quantitative CT color mapping of the arterial enhancement fraction of the liver to detect hepatocellular carcinoma. Radiology 2009;250:425–34.
[10] Fournier LS, Cuenod CA, de Bazelaire C, et al. Early modifications of hepatic perfusion measured by functional CT in a rat model of hepatocellular carcinoma using a blood pool contrast agent. Eur Radiol 2004;14:2125–33.
[11] Peterson MS, Baron RL, Marsh JWJr, et al. Pre-transplantation surveillance for possible hepatocellular carcinoma in patients with cirrhosis: epidemiology and CT-based tumor detection rate in 430 cases with surgical pathologic correlation. Radiology 2000;217:743–9.

[12] Furuse J, Maru Y, Yoshino M, et al. Assessment of arterial tumor vascularity in small hepatocellular carcinoma: comparison between color Doppler ultrasonography and radiographic imagings with contrast medium- dynamic CT, angiography, and CT hepatic arteriography. Eur J Radiol 2000;36:20–7.
[13] Bolondi L, Gaiani S, Celli N, et al. Characterization of small nodules in cirrhosis by assessment of vascularity: the problem of hypo-vascular hepatocellular carcinoma. Hepatology 2009;42:27–34.
[14] Boas FE, Kamaya A, Do B, et al. Classification of hyper-vascular liver lesions based on hepatic artery and portal vein blood supply coefficients calculated from triphasic CT scans. J Digit Imaging 2015;28:213–23.
[15] Caseiro-Alves F, Brito J, Araujo AE, et al. Liver hemangioma: common and uncommon findings and how to improve the differential diagnosis. Eur Radiol 2007;17:1544–54.
[16] António PM, Yong HJ, Miguel R, et al. Lobulated margination of liver hemangiomas: is this a definitive feature? Clin Imaging 2016;40:801–5.
[17] Valérie V, Leila B, Marie-Pierre V, et al. Imaging of atypical hemangiomas of the liver with pathologic correlation. RadioGraphics 2000;20:379–97.
[18] Winterer JT, Kotter E, Ghanem N, et al. Detection and characterization of benign focal liver lesions with multi-slice CT. Eur Radiol 2006; 16:2427–43.
[19] Woo S, Cho JY, Kim SY, et al. Histogram analysis of apparent diffusion coefficient map of diffusion-weighted MRI in endometrial cancer: a preliminary correlation study with histological grade. Acta Radiol 2014;55:1270–7.
[20] Donati OF, Mazaheri Y, Afaq A, et al. Prostate cancer aggressiveness: assessment with whole-lesion histogram analysis of the apparent diffusion coefficient. Radiology 2014;271:143–52.
[21] Suo ST, Chen XX, Fan Y, et al. Histogram analysis of apparent diffusion coefficient at 3.0 T in urinary bladder lesions: correlation with pathologic findings. Acad Radiol 2014;21:1027–34.
[22] Yang X, Knopp MV. Quantifying tumor vascular heterogeneity with dynamic contrast-enhanced magnetic resonance imaging: a review. J Biomed Biotechnol 2011;2011:732–848.
[23] Boas FE, Brody LA, Erinjeri JP, et al. Quantitative measurement of enhancement on pre-procedure triphasic CT can predict response of colorectal liver metastases to radio-embolization. Am J Roentgenol 2016;207:671–5.
[24] Cicchetti DV. Guidelines, criteria, and rules of thumb for evaluating normed and standardized assessment instruments in psychology. Psychol Assess 1994;6:284–90.
[25] Singh J, Sharma S, Aggarwal N, et al. Role of perfusion CT differentiating hemangiomas from malignant hepatic lesions. J Clin Imaging Sci 2014;4:1–7.
[26] Guo ML, Yu YM. Application of 128 slice 4D CT whole liver perfusion imaging in hepatic tumor. Cell Biochem Biophys 2014;70:173–8.
[27] Hectors SJ, Wagner M, Bane O, et al. Quantification of hepatocellular carcinoma heterogeneity with multiparametric magnetic resonance imaging. Sci Rep 2017;7:2452.
[28] Hanafusa K, Ohashi I, Himeno Y, et al. Hepatic hemangioma: findings with two-phase CT. Radiology 1995;196:465–9.
[29] Park YN, Yang CP, Fernandez GJ, et al. Neoangiogenesis and sinusoidal "capillarization" in dysplastic nodules of the liver. Am J Surg Pathol 1998;22:656–62.
[30] Ng F, Ganeshan B, Kozarski R, et al. Assessment of primary colorectal cancer heterogeneity by using whole-tumor texture analysis: contrast-enhanced CT texture as a biomarker of 5-year survival. Radiology 2013;266:177–84.
[31] Popovic P, Leban A, Kregar K, et al. Computed tomographic perfusion imaging for the prediction of response and survival to transarterial chemoembolization of hepatocellular carcinoma. Radiol Oncol 2018;52: 14–22.
[32] Ippolito D, Capraro C, Casiraghi A, et al. Quantitative assessment of tumor associated neovascularization in patients with liver cirrhosis and hepatocellular carcinoma: role of dynamic-CT perfusion imaging. Eur Radiol 2012;22:803–11.
[33] Reiner CS, Goetti R, Burger IA, et al. Liver perfusion imaging in patients with primary and metastatic liver malignancy: prospective comparison between 99m Tc-MAA spect and dynamic CT perfusion. Acad Radiol 2012;19:613–9.
[34] Yang HF, Du Y, Ni JX, et al. Perfusion computed tomography evaluation of angiogenesis in liver cancer. Eur Radiol 2010;20:1424–30.
[35] Feng J, Chen J, Zhu R, et al. Prediction of early recurrence of hepatocellular carcinoma within the Milan criteria after resection. Oncotarget 2017;8:63299–310.
[36] Monzawa S, Ichikawa T, Nakajima H, et al. Dynamic CT for detecting small hepatocellular carcinoma: usefulness of delayed phase imaging. Am J Roentgenol 2007;188:147–53.